Asian Journal of Chemistry; Vol. 33, No. 4 (2021), 767-774

ASIAN JOURNAL OF CHEMISTRY

https://doi.org/10.14233/ajchem.2021.22686

DNA Inhibition of Hydrogen Ion-Induced Corrosion of Mild Steel Used for Pipelines in Oil and Gas Industries

OLURANTI AGBOOLA[1,2,*], TOLUWANI ADEDOYIN[1], OJO SUNDAY ISAAC FAYOMI[3], AYOOLA AYODEJI[1], SAMUEL E. SANNI[1], AUGUSTINE OMONIYIN AYENI[1], PATRICIA POPOOLA[2], ROTIMI SADIKU[2], PETER ADENIYI ALABA[4], GODWIN I. AKANDE[5] and EMMANUEL EMEKA OKORO[6]

[1]Department of Chemical Engineering, Covenant University, Ota, Nigeria
[2]Department of Chemical, Metallurgical and Materials Engineering, Tshwane University of Technology, Pretoria, South Africa
[3]Department of Mechanical and Biomedical Engineering, Bells University of Technology, P.M.B 1015, Ota, Ogun State, Nigeria
[4]Department of Chemical Engineering, University of Malaya, 50603 Kuala Lumpur, Malaysia
[5]Department of Mechanical Engineering, University of Ibadan, Ibadan, Nigeria
[6]Department of Petroleum Engineering, Covenant University, Ota, Nigeria

*Corresponding author: Email: funmi2406@gmail.com; osfayomi@bellsuniversity.edu.ng

Received: 20 February 2020; *Accepted*: 16 January 2021; *Published online*: 20 March 2021; AJC-20280

Corrosion of mild steel *via* chemical reaction in a corrosive environment is a problematic occurrence that is very common in oil and gas industries. Corrosion constitutes a huge part of the total costs in the production of oil and gas. Corrosion inhibitors have found interest in the scientific domain because they are mainly understood by their chemical complexes and formulations. Their utilization in small amount on metal surface used in oil and gas industries can help shield the metal from corrosion devoid of any significant alteration in the concentration of the corrosive media in the environment. An effort was made to study the possibility of using calf thymus gland DNA (CTG_{DNA}) inhibitor in chlorine induced mild steel for possible usage in piping in oil and gas industry. The SEM micrograph shows that the adsorption of the CTG_{DNA} biomacromolecules coat on the mild steel surfaces functions as a protection against HCl corrosive solution. Electrochemical study and weight loss analysis showed that the inhibitor efficiency (70.48 and 72%, respectively) of the tested DNA (CTG_{DNA}) in HCl acidic corrosion environment for the mild steel was high at 1.5 M of HCl. The inhibitor efficiency decreased with increasing HCl concentrations. The open circuit potential (OPC) revealed that the mild steels got corroded until the end of the immersion. The intensities of XRD peak substantiate the existence of corrosion products of $FeCl_2$.

Keywords: Calf thymus gland DNA, Mild steel, Corrosion rate, Inhibitor efficiency, Open circuit potential.

INTRODUCTION

The selection of material is one of the important factors of every industry. Hence, extreme considerations are given to industrial designs of materials in order to guarantee maximum efficiency and effectiveness from their applications [1]. Mild steel is a carbon steel which contains up to 0.3% carbon and known to be an imperative engineering component, which performs an extensive variety of industrial applications. Mild steel is used in petroleum production and refining industries, chemical processing, chemical storage tank, mining and transmission pipelines, *etc.* [2]. Mild steel is generally among the most common materials employed for petroleum pipelines as a result of its distinctive physical characteristics such as ductility, weldability, enormous strength, its amenability to heat treatment for several mechanical properties and low cost [2,3].

Corrosion is a damaging outbreak of a material through reaction with its milieu [4] and a likely possible menace related to the production of oil and gas, including their conveyance facilities [5]. Nearly all aqueous milieu have the capacity to promote corrosion. Corrosion takes place under several intricate circumstances in the production of oil and gas, processing and pipeline structures [6]. Crude oil and natural gas have the capacity to carry numerous intrinsically corrosive high-impurity products [7]. For example, crude petroleum comprises of sulfur compounds. Many of these compounds are extracted in the

course of refining process. Nonetheless, there is usually some residual sulfur compounds in the petroleum product, which have the capacity to corrode a number of metals. The consequence is dependent on the types of chemical sulfur compounds present [8]. With respect to oil and gas wells and pipelines, carbon dioxide, hydrogen sulfide and free water are the highly corrosive media [9]. In addition, oil well stimulation, typically accomplished with hot solutions of hydrochloric acid, have the tendency of inducing austere corrosion outbreak on production tubing, downhole tools and casing [10]. Furthermore, the pumping of strong acids solutions, such as HCl, into the reservoir cannot be possible without the addition of efficient corrosion inhibitors to avoid the hazard of destroying pipes and well equipment by the acid [11]. There is an advantage of using HCl above the other acidic minerals in the acidizing operation of oil and gas industries. This is because HCl produces metal chlorides with solubility properties in the aqueous phase. Stereotypically, extremely concentrated hydrochloric acids in the range of 5 and 28 wt.%, are applicable in oil and gas industries; hence, the reason for corrosive environment to steels, such as carbon, mild and low-alloy steels. HCl is introduced into the well in the course of the acidizing stimulation process and lead to severe corrosion problems [12]. During the course of acidizing stimulation process by the injection of HCl, the electrochemical complexity of corrosion could be demonstrated through the strike of iron in HCl. Once iron is immersed in acid, a strong reaction takes place; consequently, hydrogen gas is evolved and iron gets dissolved. Thus, the reaction is [13]:

$$Fe + 2H^+ \longrightarrow Fe^{2+} + H_2 \quad (1)$$

The reaction in eqn. 1 can be divided into two partial reactions:

$$Fe \longrightarrow Fe^{2+} + 2e^- \quad \text{oxidation (anodic reaction)} \quad (2)$$

$$2H^+ + 2e^- \longrightarrow H_2 \quad \text{reduction (cathodic reaction)} \quad (3)$$

Wells and pipelines internal corrosion is based on several factors such as temperature, water chemistry, flow velocity, oil or water wetting, composition of the steel and the surface condition of the steel [14]. The reaction rate of the acid in the formation stimulation is a significant factor considered to influence corrosion in acid stimulation. This reaction rate depends on acid type, acid concentration, temperature, fluid velocity and formation material type [10]. Other factors are presence of oxygen, nature of the acid anion, effect of corrosion inhibitor and hydrocarbon (wax, crude oil and gas condensate).

Without the use of corrosion inhibitors, the over-all rate of corrosion could be tremendously high (>100 mm/year) and could exponentially upsurge *via* increase in temperatures and acid concentrations [15]. Combating corrosion in oilfield applications is very important, in view of the fact that the problems of corrosion yearly represent an enormous quota of the total costs for oil and gas producing industries, globally. Besides, suitable corrosion control could assist in preventing numerous possible calamities that could result in severe issues such as loss of life, negative social influences and water resource and ecological contamination [12]. The application of corrosion inhibitors has always been a first-line of protector measure against internal corrosion of equipment used in the production of oil and gas [16]. There is recently a new prospect in the use of organic inhibitor caused by the invention of DNA inhibitor, which has also led to enhanced anchoring of highly specific biological recognition of DNA elements, allowing unique performance in coating technology. Hu *et al.* [17] investigated that how biomacromolecule DNA corrosion inhibitor influences carbon steel. The chemisorption of DNA inhibitor on carbon steel surface was observed to have occurred from single-molecular-layer self-assembly. Agboola *et al.* [18] looked into the application of extracted DNA from calf thymus gland as a shield for 3CR12 stainless steel in HCl medium. An inhibition mechanism was proposed and verified by XRD analysis. Their data showed that the efficiency of corrosion inhibition rises as the HCl concentration increases. Agboola *et al.* [19] also investigated the performance of several concentrations of DNA from *Manihot esculenta* leaf (Cassava leaf) used as corrosion inhibition for mild steel in an acidic milieu. The study was done at different temperatures and found that the presence of the DNA inhibitor slowed down the corrosion process. This study proposed the possibility of applying calf thymus gland DNA (CTG_{DNA}) inhibitor to study the corrosion of chlorine induced mild steel for possible application in piping in oil and gas industries. Hence, lessening or stopping corrosion in piping in oil and gas industries can be accomplished by the inclusion of corrosion inhibitor in small concentrations to a corrosive environment [20].

EXPERIMENTAL

Extraction of DNA from thymus gland: The choice of DNA used in this study is the DNA of a calf thymus gland (CTG_{DNA}). The thymus gland was sourced from a calf acquired from an indigenous trader in a slaughterhouse, Ogun state, Nigeria. The ethanol, propanone, ethyl alcohol, ammonium acetate and HCl utilized were of analytical grade and procured from Sigma-Aldrich, USA. The thymus gland was washed and cut into smaller pieces after the removal of fats. A small portion of distilled water was added to the thymus gland in a beaker and then transferred into a blender to blend the pieces of DNA gland into a puree paste. A CTAB buffer solution (10 mL) was added to the puree paste incubated at 37 ºC for 72 h and then was spun at 4000 rpm for 15 min. The upper layer *i.e.* the supernatant was carefully poured of the tubes into 6 other tubes while the residue was discarded. The chloroform/isoamyl alcohol (6.25 mL) in the ratio of 25:1 was poured into the tubes containing the supernatant and spun at 4000 rpm for 15 min. The aqueous phase *i.e.* the supernatant or upper layer was removed and the step above was repeated again with the aqueous layer, also recovered in different set of tubes. Ammonium acetate (1.25 mL) was then pipetted into the tubes and ice cold absolute ethanol (12.5 mL) was also added. At the stage, the DNA have precipitated by the cloudy solution observed. The tubes were spun at 4000 rpm for 5 min and the DNA pellet was seen to have formed at the bottom of the tubes. The supernatant was poured out in the opposite direction of the slanting DNA pellet. The CTG_{DNA} pellet in the tube was

transferred into an incubator, operated for 15 min, at ~ 37 ºC to dry. After which their concentration were measured. The measurement of the concentration of the CTG_{DNA} extracted was done using a Nanodrop Spectrophotometer, in unit of nanogram per microliter. This extracted CTG_{DNA} was diluted to concentrations of 20 mg CTG_{DNA}/L of distilled water.

Mild steel: The metal coupons used for the corrosion experiment were mild steels (low carbon steels). They were cut in strips of equal dimension 10 mm × 10 mm × 2 mm. The composition of the mild steel coupons employed in this study are given in Table-1. The desiccant absorbed water from the air in the desiccator and kept the material on the disc in order to prevent it from getting wet or humid. The desiccator was employed to dry the metal after washing before the metal was used for the experiment and after the completion of the experiment.

Corrosion experiment: 12 M HCl was used to prepare 1.5-4.0 M HCl by diluting with distilled water. The low carbon steels were washed with propanone and ethyl alcohol; and dried in desiccators, then precisely weighed. The low carbon steels weight loss experiments were accomplished by submerging the steels in the acid solution for different inhibition concentrations and temperatures. The low carbon steels were submerged in 1.5-4.0 M HCl solution in 250 mL beakers for 8 h and the beakers were placed in a constant temperature (10 ºC) water bath. The low carbon steels were taken out, rinsed with deionized water, propanone and ethanol, dried in desiccators and reweighed using a digital weighing balance. The corrosion rate (CR) and the percentage inhibition efficiency (%IE) were obtained from eqns. 4 and 5:

$$CR = \frac{W_A - W_P}{SA \times t} \quad (4)$$

$$IE\ (\%) = \frac{CR - CR^*}{CR} \times 100 \quad (5)$$

where W_A and W_P are the weights of the low carbon steels with and without CTG_{DNA} inhibitor, correspondingly, SA is the surface area (cm^2) of the low carbon steel and t is the time of dipping the steel in the corrosive media (h). CR is the corrosion rate value in the uninhibited solution and CR* is the corrosion rate value in the inhibited solution.

Polarization measurements: Polarization measurements was used to study the behaviour of corrosion of the low carbon steels in acidic solution. From the polarizations measurements, apposite points were carefully chosen *via* the Autolab software to achieve the polarization measurements for the purpose of obtaining the polarization resistance, which was employed to compute the inhibition efficiency employing eqn. 6. The potentiostat transmits signals from the electrode system to the software that helps to interpret them to graphs. The electrode system is made of a three-electrode system that consists of the working electrode (low carbon steel), contact electrode (graphite) and the reference electrode called a calomel glass electrode (KCl).

$$\eta\ (\%) = \frac{R_p - R_p^*}{C_p} \times 100 \quad (6)$$

where η % represents the efficiency of inhibitor, R_p and R_p^* represent the polarization resistance with and without inhibitor respectively.

Morphological characterization of low carbon steel: The microstructure of the surface of low carbon steel submerged in the acidic solution was evaluated using scanning electron microscopy (SEM). The elemental composition and content of corrosion products on the low carbon steel surface were achieved using element mapping.

XRD studies: The XRD was employed to identify the crystallographic phases of the metals. WAXD Pan Analytical Xpert′Pro diffractometer with the aid of CuKα radiation together with a wavelength of 0.15 nm with a goniometer radius of 240 mm, a voltage of 45 kV and a current 40 mA was used for the XRD study of the low carbon steel samples.

RESULTS AND DISCUSSION

SEM and EDS analysis of mild steel in the absence of CTG_{DNA} inhibitor: The scanning electron microscopy of the mild steels was done in order to study the structure and the morphology of mild steel without the inhibitor in the corrosive medium at 10 ºC for 1.5-4.0 M HCl concentration. Fig. 1 depicts that the mild steel surface got damaged after immersion in HCl for all concentrations of HCl without the inhibitor, in response to elevated rate of dissolution of ion in HCl solution [19]. The confirmation of the elemental composition of mild steel surface in the absence of CTG_{DNA} inhibitor in 1.5-4.0 M HCl was obtained from EDX analysis. The EDX spectra, which gives an illustration that the mild steel surface in the absence of inhibitor, reveals the presence of chloride content as a result of the corrosive outbreak of HCl (Fig. 2). The magnitude in which the mild steel got damaged increases with increasing concentration of HCl *i.e.* the surfaces of the mild steel tend to be rougher as the concentration increases. The EDS shows that the immersion of the mild steel in higher HCl concentration results in higher the wt.% of chlorine on the surface of the mild steel.

SEM and EDS analysis of mild steel in the presence of CTG-DNA inhibitor: Fig. 3 shows the observation of the CTG_{DNA} inhibitor on the mild steel surfaces at different concentrations with the utilization of the CTG_{DNA} inhibitor at 10 ºC for 8 h. It depicts that the adsorption of CTG_{DNA} biomacromolecules coat on the mild steel surfaces serves as a shield against HCl solution. Nonetheless, the higher the concentration, the more porous the surface of the mild steel. Mild steels dipped in 1.5-2.5 M HCl have less porosity, while the immersion of mild steel in 2.5-4.0 M HCl have more porosity. It is hence, envisaged that the higher the concentration of HCl, the damaged the deposition of CTG_{DNA} inhibitor on mild steel. Porosity can be instigated by damaged deposition. Damaged deposition point

TABLE-1
COMPOSITION OF THE MILD STEEL COUPON [Ref. 18]

Element	Fe	C	Si	Mn	Al	Cr	P	S	Ni
Composition (%)	99.2	0.15	0.17	0.43	0.006	0.001	0.02	0.033	0.007

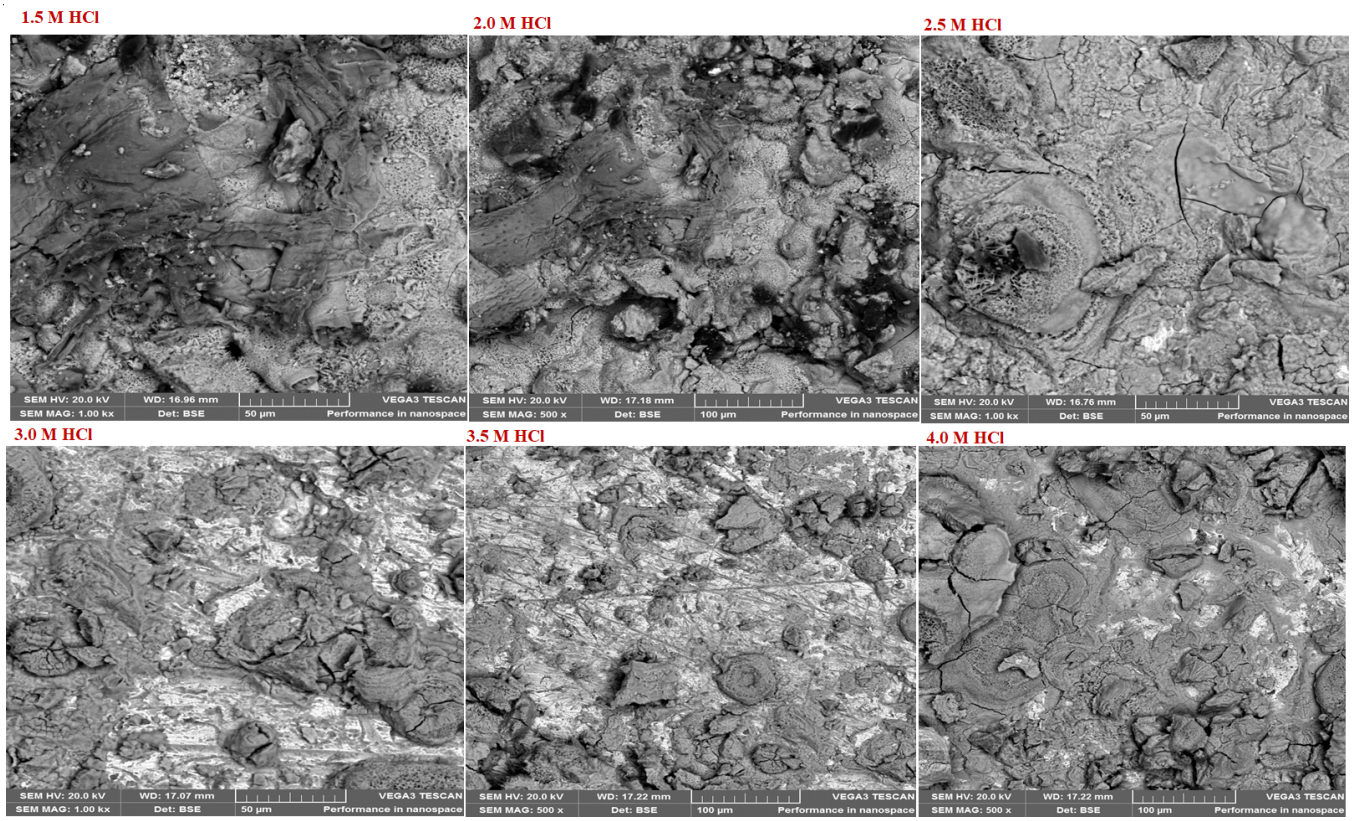

Fig. 1. SEM of the mild steel without CTG_{DNA} inhibitor at different concentrations of HCl

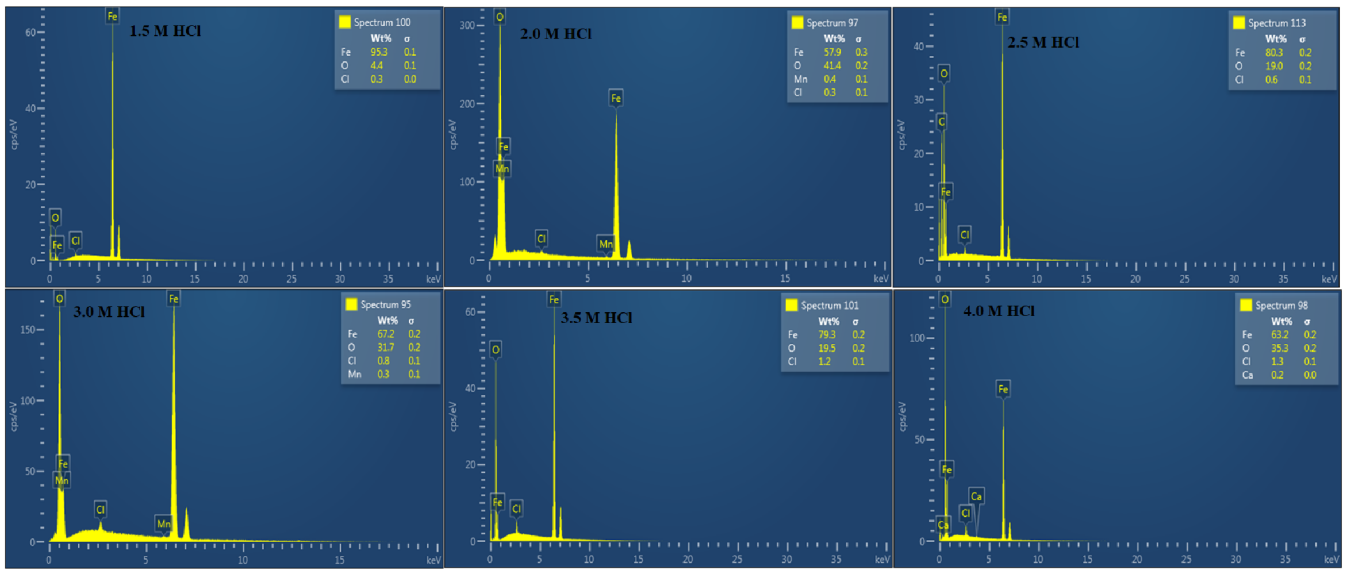

Fig. 2. EDS Spectra of the mild steel surfaces without CTG_{DNA} inhibitor at different concentrations of HCl

out that the coating process is unable to coat the entire surface of the mild steel at higher concentration of HCl. Hence, the higher the concentration of HCl the faster the corrosion rate [21]. In addition, a higher concentration of acid increases the pores and pore sizes that are created during gravimetric process, this could lead to etching process [22]. It was proven from the micrograph image in Fig. 3 that a high corrosion inhibition efficiency of CTG_{DNA} inhibitor in HCl milieu was attained at lower concentrations of HCl.

Fig. 4 shows that mild steel is inhibited in 1.5-2.5 M HCl solution as the EDS of the surfaces show no chloride content, therefore the integration of CTG_{DNA} inhibitors to the HCl solution at lower concentrations curtailed acidic occurrence on mild stainless steel [23]. However, EDS of the surfaces mild steel showed chloride content, which increases as the concentration of HCl media increases. This serve as a confirmation that at higher the concentrations of HCl, the deposition of CTG_{DNA} inhibitor on mild steel got damaged, which resulted

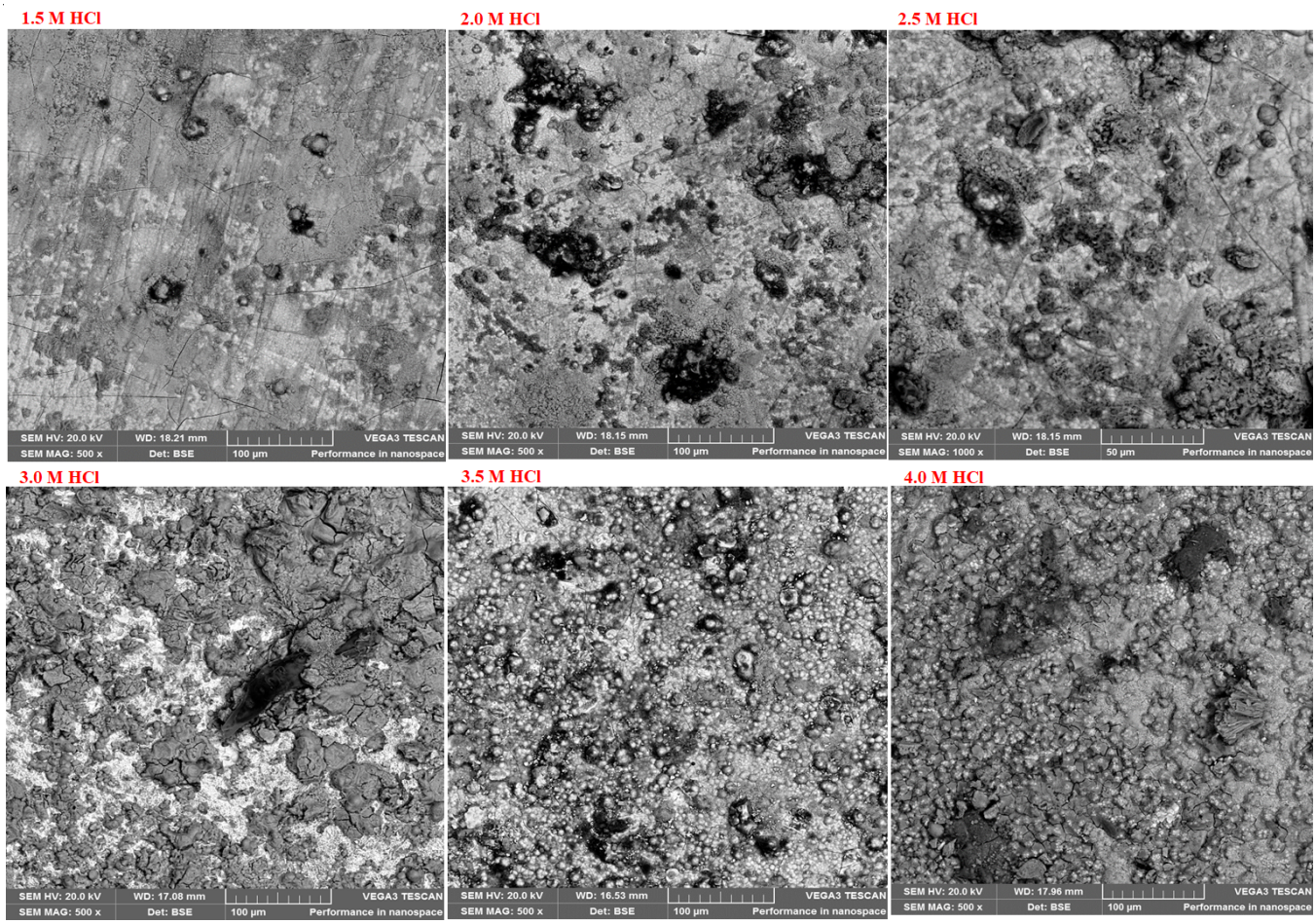

Fig. 3. SEM of the mild steel with CTG_{DNA} inhibitor at different concentrations of HCl

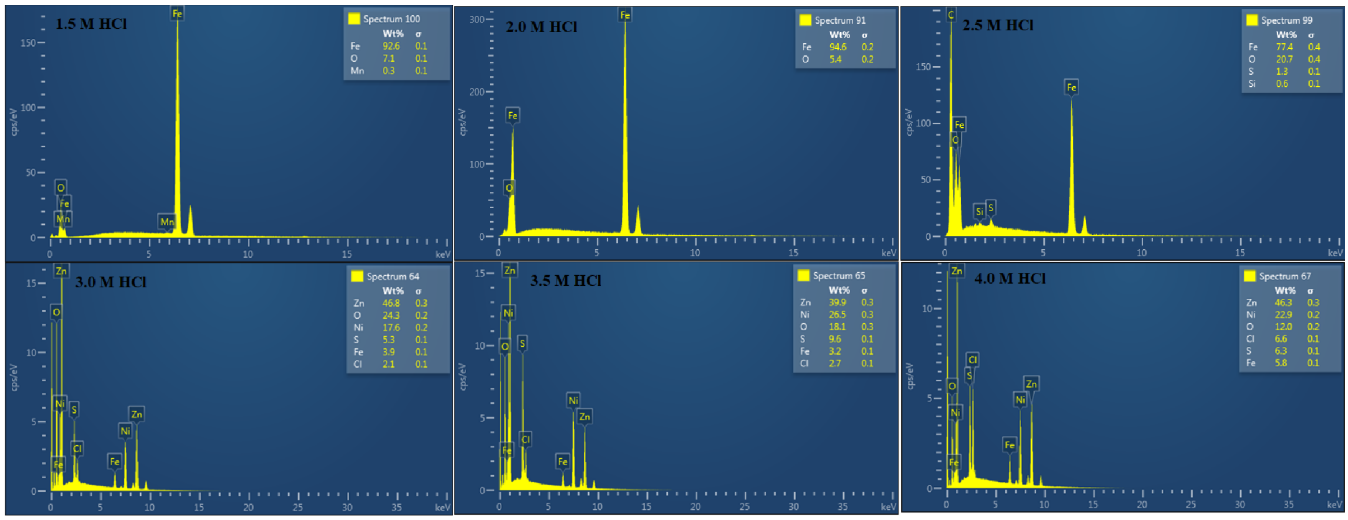

Fig. 4. EDS spectra of the mild steel surfaces with CTG_{DNA} inhibitor at different concentrations of HCl

in increasing porosity. The main reason is that the active species (*i.e.* quantities of hydrogen ions) are increased, as acid concentration is increased [24].

Study of weight loss: The study of weight loss was done at increasing concentrations of HCl for the purpose of validating the protective ability of CTG_{DNA} inhibitor on mild steel with increasing concentration of acidic environment, since higher concentrated hydrochloric acid are used in oil and gas industries. However, the highest inhibitor efficiency was obtained at 1.5 M HCl (68.57%) as shown in Table-2. The weight loss data of the mild steel samples with and without 20 mg L^{-1} CTG_{DNA} inhibitor concentration at 10 ºC with increasing concentrations of HCl is shown in Table-2. The conditions of analysis were based on the established fact that the higher inhi-

TABLE-2
GRAVIMETRIC ANALYSIS BLANK AND 20 mg L^{-1} OF CTG_{DNA} INHIBITOR AT 10 °C FOR INCREASING CONCENTRATIONS OF HCl

Molarity of HCl (M)	Without CTG_{DNA} inhibitor					In presence of CTG_{DNA} inhibitor (20 mg L^{-1})					
	Weight (mg)			CR (mg/cm^2 h)	IE (%)	Weight (mg)			CR (mg/cm^2 h)	Drop in CR	IE (%)
	Before	After	Loss			Before	After	Loss			
1.5	2198.4	2190.6	7.8	780	0	2207	2204.8	2.2	220	560	72.00
2.0	2349.7	2338.9	10.1	1010	0	2124.7	2120.4	4.3	430	580	57.43
2.5	2504.3	2491.6	12.7	1270	0	2329	2322.6	6.4	640	630	49.61
3.0	2071.8	2057.6	14.2	1420	0	2255.4	2247.0	8.4	840	580	40.85
3.5	2415.8	2399.2	16.6	1660	0	2215.4	2204.2	11.2	1120	540	32.53
4.0	2434.9	2416.9	18.0	1800	0	2110.5	2096.8	13.7	1370	430	23.89

CR = Corrosion rate; IE = Inhibition efficiency

bitor concentration at lower temperature favours the utilization of DNA as corrosion inhibitor [18,19]. Table-2 shows that the corrosion continued to drop from 480-630 mg/cm^2 h for 1.5-2.5 M HCl. The continuous drop in the corrosion rate of the mild metal from 1.5-2.5 M may be attributed to the creation of a denser shielding layer at higher concentrations (Fig. 5). However, there was continuous rise in the corrosion rate of the mild metal from 1.5-2.5 M, which can be attributed due to the deposition of CTG_{DNA} inhibitor on mild steel at higher concentration of HCl, which was observed in Fig. 3. Furthermore, the maximum inhibition efficiency (72%) was attained at 1.5 M of HCl and as the concentration of HCl increases, the inhibition efficiency reduces with 4.0 M of HCl having lowest inhibition efficiency (23.89%).

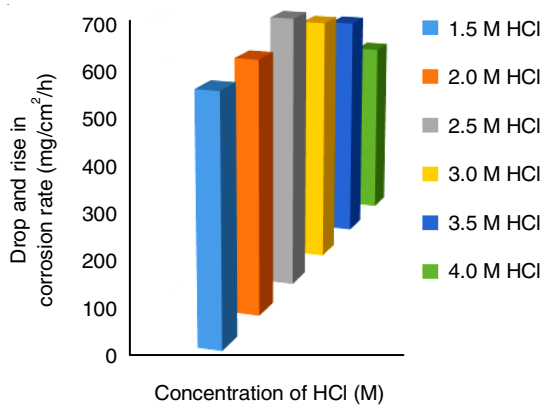

Fig. 5. Drop and rise in corrosion rate as a function of concentrations of HCl

Polarization measurement: Potentiodynamic polarization measurement of CTG_{DNA} inhibitor in 1.5-4.0 M HCl solution without and with inhibitor at 10 ºC and 20 mg/L concentrations of the CTG_{DNA} inhibitor are shown in Fig. 6. Though, the weight loss study and the potentiodynamic polarization measurement show that there was continuous drop in the corrosion rate from 1.5-2.5 M and rise corrosion rate from 3.0-4.0 M, both the cathodic and anodic processes are slowed down by adding CTG_{DNA} inhibitor for all concentrations of HCl. The core electrochemical anodic and cathodic reactions for the corrosion of mild steel in one of the corrosive species (Cl^-) found in oil fields environments are as follows [25]:

$$Fe^{2+} + 2Cl^- \longrightarrow FeCl_2 \quad (8)$$

$$FeCl_2 + 2H_2O \longrightarrow Fe(OH)_2 + 2H^+ + 2Cl^- \quad (9)$$

$$FeCl_2 + 2Cl^- \longrightarrow FeCl_3 + e^- \quad (10)$$

$$Fe + 2H^+ \longrightarrow Fe^{2+} \quad (11)$$

At high concentrations of HCl solution (3.0-4.0 M), the diffusion of atoms was fitful, which allows the transmission of reactive elements to the mild steel surface in order look for oxygen reactive sites. The O_2 molecule became weakened by the interaction with the mild steel surface [26], through the creation of vacancies in the matrix *via* the transmission from

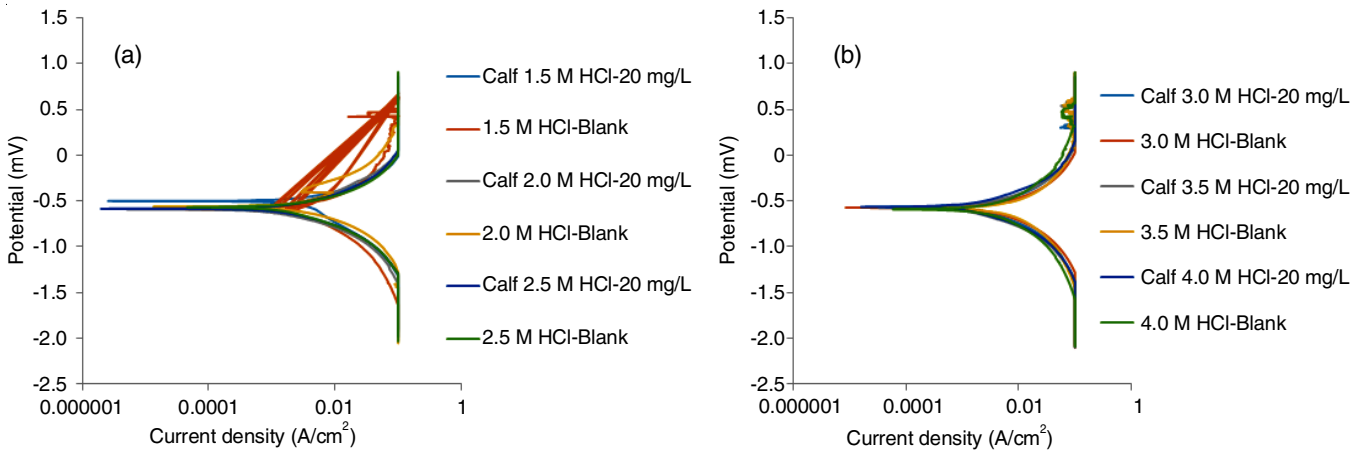

Fig. 6. Tafel polarization at 10 ºC in the presence and absence of 20 mg/L CTG_{DNA} Inhibitor for six different concentrations of HCl (1.5-4.0 M) with 0.5 interval

the lattice sites. The polarization measurements showed that the tested inhibitor is a mixed inhibitor (Table-3). The highest inhibition efficiency obtained at 1.5 M HCl concentration is 70.48%. This inhibition efficiency has a close agreement with the value obtained from the weight loss (72%). The inhibition efficiency decreases with an increase in HCl concentration (1.5-4.0 M). Hence, the corrosion rate increases at high concentration of HCl, which implies that Cl^- ions strike Fe/Fe^{2+} to form corrosion products $FeCl_2$ and $FeCl_3$ as shown in equations 8 and 10. $FeCl_2$ is not stable and could hydrolyze or react further with Cl^- ions to form $Fe(OH)_2$ or $FeCl_3$ (eqns. 9 and 10, respectively). This result is in accordance with the findings of Fontana & Green [24]. A study has shown that the adsorption of CTG_{DNA} inhibitors on metal steel could be attributed to the electrostatic interaction that takes place between the negatively charged surface of the steel and the positive charge inhibitor molecule or through the dissemination of charge amid CTG_{DNA} hydrogen bonds, harmonizing organic bases and the surface [19]. However, the electrostatic interaction that took place between the negatively charged surface of the mild steel and the positive charge CTG_{DNA} inhibitor molecule was only favourable at the lower concentration of HCl. Hence, a resilient adsorption formation of film on mild steel provides good corrosion resistance at lower concentration of HCl. Formation of bond and dipole-dipole interactions were considered significant factors for film formation on mild steels at low concentration of HCl [27]. This result was affirmed by XRD surface analysis.

The open circuit potential (OCP) of mild steel in different concentration of HCl is shown in Fig. 7. This open circuit potential was done to monitors the free potential difference between working and reference electrodes when no external current is flowing in the cell. The results showed that the blank sample of bare mild steel in 1.5 M, 2.0 M and 2.5 M HCl instantly reached corrosion potentials of -0.620 V, -0.623 V and -0.600 V (*vs.* SCE) after immersion (Fig. 7a). Fig. 7b showed that the blank sample of bare mild steel in 3.0 M, 3.5 M and 4.0 M HCl instantly reached corrosion potentials of -0.627 V, -0.613 V and -0.571 V (*vs.* SCE) after immersion. Thus, mild steels were considered corroded until the end of the immersion. This result is comparable to the work investigated by Martyak & McAndrew [28], whereby chloride ion quickly corrodes uncoated or uninhibited mild steel at a mild steel corrosion potential of -0.60 V. However, all the corrosion potential possess similar trend. The potentials increases until the passive film stretches to its limiting protective capacity, bringing about stabilization of the corrosion potential at about 120 s. Hence, the electrochemical reactions at mild steel electrolyte interface vary with time [29]. The potentials begin to slowly drift to the more negative direction; for example, with 4 M HCl (20 mg/L CTG_{DNA} inhibitor) at -0.646 mV, while increase in less negative direction to -0.614 mV at about 34 s, then reach the maximum stabilization potential at -0.61 mV at 120 s.

XRD analysis of corrosion products on the surfaces of mild steel: Fig. 8 shows the XRD patterns with 20 mg/L of CTG_{DNA} inhibitor and without CTG_{DNA} inhibitor for different concentration of HCl at 10 ºC. The crystallographic phases on each sample of mild steel and the alignment of these crystals on the steel can be detected. The intensity of uninhibited samples were low at all concentrations of HCl; however, the intensity of higher concentrations of HCl (3.0-4.0 M HCl) was higher than the intensity of lower concentrations of HCl (1.5-2.5 M HCl). The existence of corrosion products of $FeCl_2$ and $FeCl_3$ is evidently shown by the XRD peak intensities. This result corroborates with the corrosion rate and decrease in the

TABLE-3
ELECTROCHEMICAL CORROSION PARAMETERS IN BLANK AND 20 mg L^{-1} OF CTG_{DNA} INHIBITOR AT 10 °C FOR INCREASING CONCENTRATIONS OF HCl

Samples in HCl (M)	Without CTG_{DNA} inhibitor				In presence of CTG_{DNA} inhibitor (20 mg L^{-1})				
	E_{corr} (mV)	J_{corr} (A/cm^2)	CR (mm/year)	PR (Ω)	E_{corr} (mV)	J_{corr} (A/cm^2)	CR (mm/year)	PR (Ω)	IE (%)
1.5	-0.58928	0.00046067	10.553	24.180	-0.50178	0.00030480	3.1148	14.599	70.48
2.0	-0.59345	0.00060353	9.0130	21.009	-0.59265	0.00037225	4.3255	39.894	52.00
2.5	-0.58770	0.00072854	8.4656	26.228	-0.58462	0.00054080	4.9841	29.639	41.12
3.0	-0.57272	0.00150130	14.021	14.120	-0.56656	0.00071657	7.8260	21.991	44.18
3.5	-0.58144	0.00346960	13.617	10.790	-0574680	0.00081045	9.4174	32.198	30.84
4.0	-0.59106	0.00371720	15.194	19.113	-0.56519	0.00100280	11.652	34.438	23.31

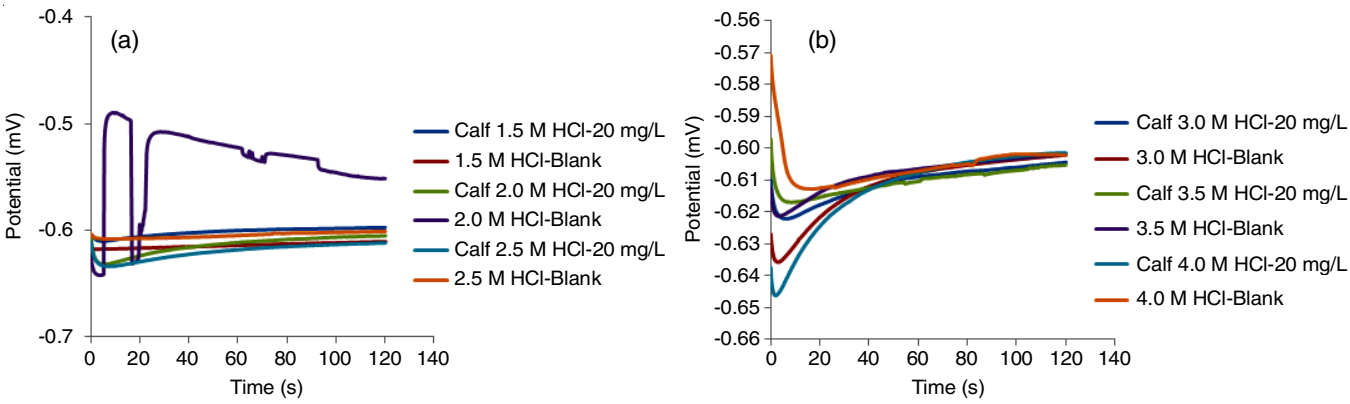

Fig. 7. Open circuit potential (OCP) of the mild steel in different concentration of HCl

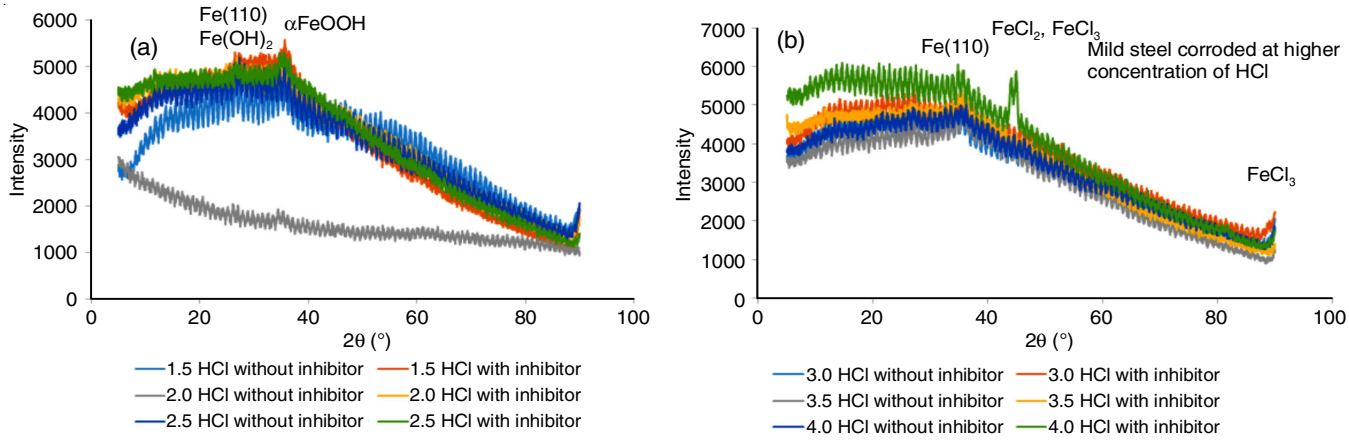

Fig. 8. XRD spectrum of mild steel showing peaks of different corroded phases in (a) 1.5-2.5 M HCl and (b) (a) 3.0-4.0 M HCl in the presence of 20 mg/L of CTG DNA corrosion inhibitor at 10 ºC

corrosion efficiency as a result of Cl^- ions as found in the polarization and weight loss studies. Peaks at 2θ = 33º and 40º in Fig. 8a, can be assigned to iron and the oxides of iron while the peaks at 2θ = 44.06º and 89.86º to 89.87º in Fig. 8b can be assigned to corrosion products of $FeCl_2$ and $FeCl_3$.

Conclusion

This study is an attempt to investigate the possibility of using CTG_{DNA} inhibitor in chlorine induced mild steel for possible applications in oil and gas industry. Data obtained showed that the possibility of using CTG_{DNA} inhibitor at higher HCl acid concentration is not visible as the highest inhibition efficiency was obtained at 1.5 M of HCl. It was established that the data obtained from the polarization measurement was close to the data obtained from the weight loss analysis. The XRD peak intensities confirms the presence of corrosion products of $FeCl_2$.

CONFLICT OF INTEREST

The authors declare that there is no conflict of interests regarding the publication of this article.

REFERENCES

1. O.K. Ukoba, P.K. Oke and M.C. Ibegbulam, *Int. J. Sci. Technol.*, **2**, 618 (2012).
2. M. Finšgar and J. Jackson, *Corros. Sci.*, **86**, 17 (2014); https://doi.org/10.1016/j.corsci.2014.04.044
3. W.F. Smith and J. Hashemi, Foundations of Material Science and Engineering, McGraw-Hill: New York (2006).
4. P.R. Roberge, Handbook of Corrosion Engineering, McGraw-Hill: New York (2000).
5. M.B. Kermani and L.M. Smith, CO_2 Corrosion Control in Oil and Gas Production: Design Considerations; The Institute of Materials, European Federation of Corrosion Publications: London (1997).
6. Champion Technologies, Corrosion Mitigation for Complex Environments. Champion Technologies, Houston, USA (2012).
7. M. Mansouri, H. Atashi, A. Mirzaei and R. Jangi, *Int. J. Indus. Chem.*, **4**, 1 (2013); https://doi.org/10.1186/2228-5547-4-1
8. J. Garcia-Antün, J. Monzü, L. GuiEiün, D. Gümez and J. Costa, *Fresenius J. Anal. Chem.*, **337**, 382 (1990); https://doi.org/10.1007/BF00322216
9. D. Lusk, M. Gupta, K. Boinapally and Y. Cao, *Hydrocarbon Eng.*, **13**, 115 (2008).
10. P. Rajeev, A.O. Surendranathan and Ch.S.N. Murthy, *Environ. Sci.*, **3**, 856 (2012).
11. Y.I. Kuznetsov, A.A. Chirkunov and A.M. Semiletov, *Int. J. Corros. Scale Inhib.*, **8**, 850 (2019); https://doi.org/10.17675/2305-6894-2019-8-4-5
12. M. Finsgar and J. Jackson, *Corros. Sci.*, **86**, 17 (2014); https://doi.org/10.1016/j.corsci.2014.04.044
13. N. Muthukumar, Petroleum Products Transporting Pipeline Corrosion: A Review, In: The Role of Colloidal Systems in Environmental Protection, Elsevier: UK, Chap. 21 (2014).
14. L.T. Popoola, A.S. Grema, G.K. Latinwo, B. Gutti and A.S. Balogun, *Int. J. Indus. Chem.*, **4**, 35 (2013); https://doi.org/10.1186/2228-5547-4-35
15. E. Barmatov, J. Geddes, T. Hughes and M. Nagl, Research on corrosion inhibitors acid stimulation, in: *NACE,* pp C2012–0001573 (2012).
16. M.A. Ibraheem, A.E.E. Fouda, M.T. Rashad and F.N. Sabbahy, *Int. Scholarly Res. Network,* **2012**, 892385 (2012); https://doi.org/10.5402/2012/892385
17. K. Hu, J. Zhuang, J. Ding, Z. Ma, F. Wang and X. Zeng, *Corros. Sci.*, **125**, 68 (2017); https://doi.org/10.1016/j.corsci.2017.06.004
18. O. Agboola, F. Achile, S.O. Fayomi, S.E. Sanni, O. Abatan, E.R. Sadiku, P. Popoola, M.P. Mubiayi, E.T. Akinlabi, M.E. Makhatha, T. Adedoyin and I. Ekere, *J. Bio- and Tribo-Corros.*, **5**, 52 (2019); https://doi.org/10.1007/s40735-019-0245-5
19. O. Agboola, T. Adedoyin, S.E. Sanni, E.A. Omonidgbehin, S.O. Fayomi, B.E. Adegboye, A. Ayoola, O. Omodara, A.O. Ayeni, P. Popoola, R. Sadiku and P.A. Alaba, *Anal. Bioanal. Electrochem.*, **11**, 1304 (2019).
20. O. Agboola, S.E. Sanni, S.O. Fayomi, P. Popoola, R. Sadiku, A. Adegbola and V.O. Fasiku, *J. Bio. Tribo. Corros.*, **6**, 7 (2020); https://doi.org/10.1007/s40735-019-0308-7
21. R.D. Desiati, E. Sugiarti and K.A.Z. Thosin, Effect of Cloric Acid Concentration on Corrosion Behavior of Ni/Cr Coated on Carbon Steel. Proceedings of the International Seminar on Metallurgy and Materials (ISMM2017), no. 1964, pp 1-6 (2017).
22. T.M. Martin, D.B. Robinson and R.J. Narayan, Nanoporous Gold for Biomedical Applications: Structure, Properties, and Applications, In: Precious Metals for Biomedical Applications, Cambridge: Woodhead Publishing Ltd., Chap. 7, pp. 148-162 (2014).
23. H. Hamani, T. Douadi, D. Daoud, M. Al-Noaimi, R.A. Rikkouh and S. Chafaa, *J. Electroanal. Chem.*, **801**, 425 (2017); https://doi.org/10.1016/j.jelechem.2017.08.031
24. M.G. Fontana and N.D. Green, Corrosion Engineering, McGraw-Hill Publication, USA, ed. 2 (1978).
25. S. Paul, A. Pattanayak and S.K. Guchhait, *Int. J. Metals*, **2014**, Article ID 628505 (2014); https://doi.org/10.1155/2014/628505
26. A. Ruiz Puigdollers, P. Schlexer, S. Tosoni and G. Pacchioni, *ACS Catal.*, **7**, 6493 (2017); https://doi.org/10.1021/acscatal.7b01913
27. D. Dwivedi, K. Lepkova and T. Becker, *RSC Advances*, **7**, 4580 (2017); https://doi.org/10.1039/C6RA25094G
28. N.M. Martyak and P. McAndrew, *Corros. Sci.*, **49**, 3826 (2007); https://doi.org/10.1016/j.corsci.2007.05.013
29. O.S. Shehata, L.A. Khorshed and H.S. Mandour, *Egypt. J. Chem.*, **60**, 243 (2017); https://doi.org/10.21608/EJCHEM.2017.674.1014